Available online at www.sciencedirect.com
SCIENCE DIRECT®
Journal of Non-Crystalline Solids 349 (2004) 38–45
JOURNAL OF NON-CRYSTALLINE SOLIDS
www.elsevier.com/locate/jnoncrysol

Structural changes of various types of silica glass tube upon blowing with hydrogen–oxygen flame

Yosuke Kokubo [a], Nobu Kuzuu [b,c,*], Izumi Serizawa [a], Ling-Hai Zeng [b], Kenji Fujii [b]

[a] *ORC Manufacturing Co. Ltd., 4896 Tamagawa, Chino-shi, Nagano 391-0011, Japan*
[b] *Department of Applied Physics, University of Fukui, 3-9-1 Bunkyo, Fukui-shi, Fukui 910-8507, Japan*
[c] *Fukui Prefecture Collaboration of Regional Entities for the Advancement of Technology Corporation, 61 Kawai Washizuka-cho, Fukui-shi, Fukui 910-0102, Japan*

Available online 28 October 2004

Abstract

Structural changes upon blowing with a hydrogen–oxygen flame were examined in three types of silica glass tube, containing <1, 200, and 1300 ppm of OH (referred to as Samples I, II and III, respectively). The samples were studied by means of microscopic spectroscopy. Upon blowing, the OH concentration near the outside surfaces of Samples I and II increased, whereas that near the outside surface of Sample III decreased. On the basis of an analysis of the SiOH absorption band (by peak decomposition), changes in the distribution of free SiOH, H_2O molecules, and hydrogen-bonded SiOH are discussed. The silica tube with a higher OH content has a lower fictive temperature as indicated by an IR absorption peak near 2260 cm^{-1}. After blowing, the fictive temperature of Samples II and III remained almost constant throughout the cross-section, while that of Sample I changed, ranging from 1400 to 1700 K. The maximum fictive temperature was found at a depth of approximately 1000 μm from the outside surface.

PACS: 61.43.Fs; 7.40.Pg

1. Introduction

Vitreous silica (v-SiO_2) is a high-purity amorphous silicon dioxide (SiO_2). This material can be divided into synthetic fused silica (SFS), produced from liquid material in the vapor phase or liquid phase, and fused quartz (FQ) produced by melting natural quartz powder [1]. Fused quartz can be further divided into two categories. One is type-I FQ produced by melting natural quartz powder in an electronic furnace or by an arc plasma, which contains at most ≈40 ppm of OH. The other is type-II FQ produced by melting quartz powder in a hydrogen–oxygen flame. In recent decades, the structures and properties of SFS have been studied extensively [2–4], stimulated by the development of the technologies of optical telecommunication and lithography for ultralarge-scale integrated circuits (ULSIs). In these applications, SFS is used as optical fibers, photomasks and lenses for a step-and-repeat projector (a stepper). Bulbs of high-intensity discharge (HID) lamps are fabricated by blowing type-I FQ with a hydrogen–oxygen flame. The structure of silica glass, particularly the OH-related structure, is changed by the blowing process. We examined, in a previous study [5], the change of the OH content distribution in a type-I FQ tube upon blowing, and found that the OH content increases at a depth of approximately 1000 μm from the outer surface. We also examined the change of the fictive temperature distribution.

Although OH-free FQ are used in HID lamp bulbs, utilizing the effect of the OH structure on their durability against the fabrication processing and lightening of the

* Corresponding author. Tel.: +81 776 27 8664; fax: +81 776 27 8750.
E-mail address: kuzuu@polymer.apphy.fukui-u.ac.jp (N. Kuzuu).

0022-3093/$ - see front matter © 2004 Elsevier B.V. All rights reserved.
doi:10.1016/j.jnoncrysol.2004.08.260

lamp might be necessary to improve the lifetime of the HID lamp. For example, SiOH improves the ultraviolet (UV) laser resistivity; the intensities of ArF- and KrF-excimer-laser induced absorption decrease with increasing OH contents [6,7]. In a previous work, one of the present authors and his colleagues studied the effect of heating on the structural change of a type-III fused silica containing approximately 1500 ppm of OH [8]. Upon heating at 1433 K for 120 h in ambient atmosphere, the OH content decreased by at most 70 ppm from a few centimeters from the surface, and UV absorption bands due to the defect structures are induced. If we use OH-containing silica as a bulb material for HID lamps, the effect of heating on the decrement of OH content and the effect of fusing by a hydrogen–oxygen flame on the increment of OH content might be balanced. Therefore, in this work we studied the change of OH content and distribution upon blowing in silica glass tubes containing OH.

2. Experimental procedure

Samples used in this study are listed in Table 1. Samples I, II, and III are commercially available silica glass tubes, being General Electric GE214 and Tosoh Quartz N and ES grades, respectively. These silica glass tubes were blown into a spherical shape using a hydrogen–oxygen flame and a glass lathe for ≈1 h as shown in Fig. 1. During the blowing process, nitrogen gas flowed through the tube for blowing and the tube was shaped spherically using a carbon tool [9].

Samples were cut from the part marked in Fig. 1 and polished on two facing surfaces; samples thickness of $d_S = 0.5$ mm were prepared for the measurement of infrared (IR) spectra. IR spectra were measured with a Jasco FT/IR 610 with a micro-20 microscopic unit with an aperture size of 100×100 μm. The tube thicknesses d_T were 3.5 ± 0.5 mm, in both as-received and blown tubes. OH content was determined from the peak intensity of the absorption peak at 3672 cm^{-1} using an absorption coefficient of 77.51 $mol^{-1}\,cm^{-1}$ [10].

The degree of change of d_T in Sample II upon blowing is greater than that in the other samples (Table 1). This is because the thickness of the as-received tube for Sample II is greater than those of the other samples. In Sample I, d_T after blowing was greater than that before blowing. Since different test pieces cut from different positions in the raw material were used in the measurement, this difference may be due to variation in the tube thickness. To avoid the effect of the thickness distribution, the position in the cross-section is represented by the distance x from the outer surface (OS) in the unit of sample thickness d_T.

Table 1
Samples used in this study

Sample	Type	OH content ppm		Thickness mm	
		As-received	Blown	As-received	Blown
I	Type-I FQ	<1	42	3.50	3.70
II	Type-II FQ	200	242	4.00	3.35
III	Type-III SFS	1300	1240	3.25	3.05

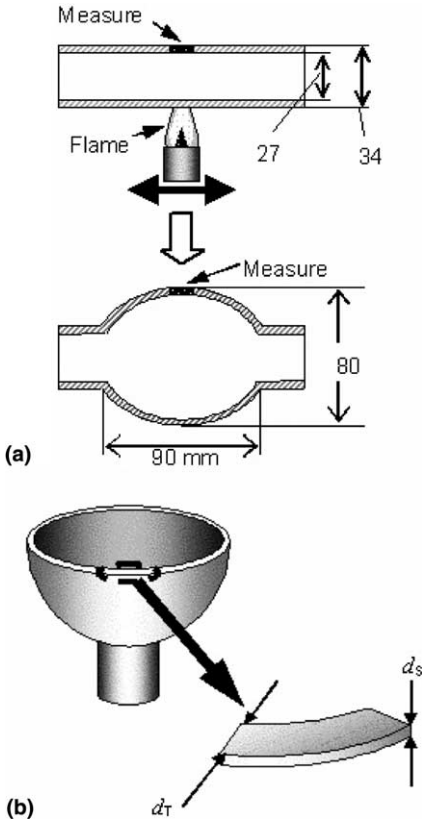

Fig. 1. (a) Blowing process of silica glass tube and (b) the sampling method.

3. Results

3.1. Change of OH distribution on blowing

Infrared (IR) absorption spectra of hydroxyl groups at several points in the cross-section of Sample I are shown in Fig. 2. The distributions of OH content before and after blowing are shown in Fig. 3. The OH contents in both Samples I and II increased steeply with increasing proximity to the surface. The character of the OH content distribution change in Sample III was different from that in the other samples. The OH content in Sample III near the inner surface (IS) increased slightly, while it decreased steeply with increasing proximity to the OS.

Forms of hydroxyl, i.e., free SiOH, hydrogen-bonded OH and H_2O molecules, can be distinguished by the peak decomposition of the IR absorption band.

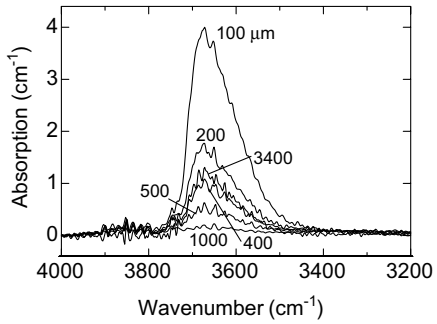

Fig. 2. Examples of OH absorption spectra near 3600 cm^{-1} at several points in the cross-section in Sample I.

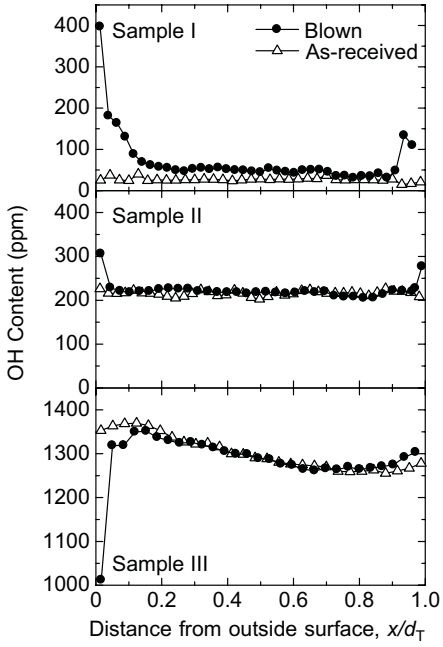

Fig. 3. Distribution of the OH content in the cross-section of silica glass tubes before and after blowing.

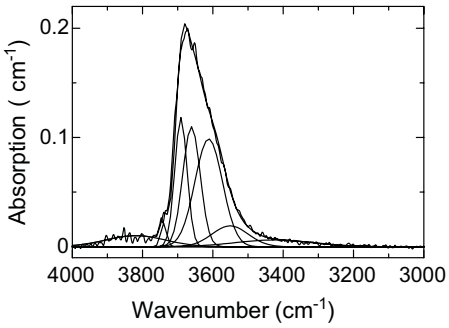

Fig. 4. Example of the peak decomposition of OH absorption.

Table 2
Absorption components used for the peak decomposition of OH absorption near 3600 cm^{-1}

Peak (cm^{-1})	FWHM (cm^{-1})	
3250	220	H_2O
3246	261	H_2O
3551	121	H-bonded
3612	92	Free OH
3661	58	Free OH
3691	41	Free OH
3740	20	Unknown
3820	200	H_2O

Although these absorption components are not exactly Gaussian, [11] we used Gaussian absorption components because these components are sufficiently similar to Gaussian ones [5] (see Fig. 4). Peak positions and full widths at half maxima (FWHMs) in each component are shown in Table 2.

The distributions of the peak intensities of each type of OH are shown in Fig. 5. Regarding free SiOH, only the 3661 cm^{-1} component is indicated in Fig. 5 because the other free-SiOH components at 3612 and 3691 cm^{-1} are distributed in the same manner as this peak, as was pointed out in the previous study [5]. The distribution of free SiOH is almost the same as the OH content distribution shown in Fig. 3, because free SiOH is dominant among all types of hydroxyls.

Absorption bands at 3250 and 3426 cm^{-1} are due to the presence of H_2O molecules [5,12]. Since these components are weak and exist in the tail of OH absorption, the result of the peak decomposition contains considerable error. The error is considered to be caused by the manner of the determination of the baseline and the adoption of the Gaussian approximation. The reliability of the 3250 cm^{-1} band must be poorer than that of the 3426 cm^{-1} band because the 3250 cm^{-1} band exists further from the OH absorption peak and its intensity is weaker than that of the 3426 cm^{-1} band. Even when we used the 3426 cm^{-1} band, the result was considered to contain considerable error, but the distribution may not so different from the exact one. Therefore, only the 3426 cm^{-1} band intensities are indicated as being those of the H_2O component in Fig. 5. The intensities of the H_2O component in Sample I are weak compared to those in the other samples. The number of H_2O molecules in Sample I increased within approximately 500 μm ($x/d_T \approx 0.13$) of the OS upon blowing. On the other hand, the intensity of the H_2O absorption component near the IS decreased. The ratio of the peak intensities of H_2O to free SiOH components in Sample I which ranged between 2.0 and 3.3 before blowing, decreased to 0–1.5 after blowing (Fig. 6(a)). The ratio after blowing approaches zero at both surfaces. This is due to the increment of the free OH content at both surfaces after blowing, because the increment near the OS and a slight decrement near the IS were observed, as shown in Fig. 5(b).

In Sample II, in the same manner, the amount of H_2O increased with increasing proximity to the OSS and

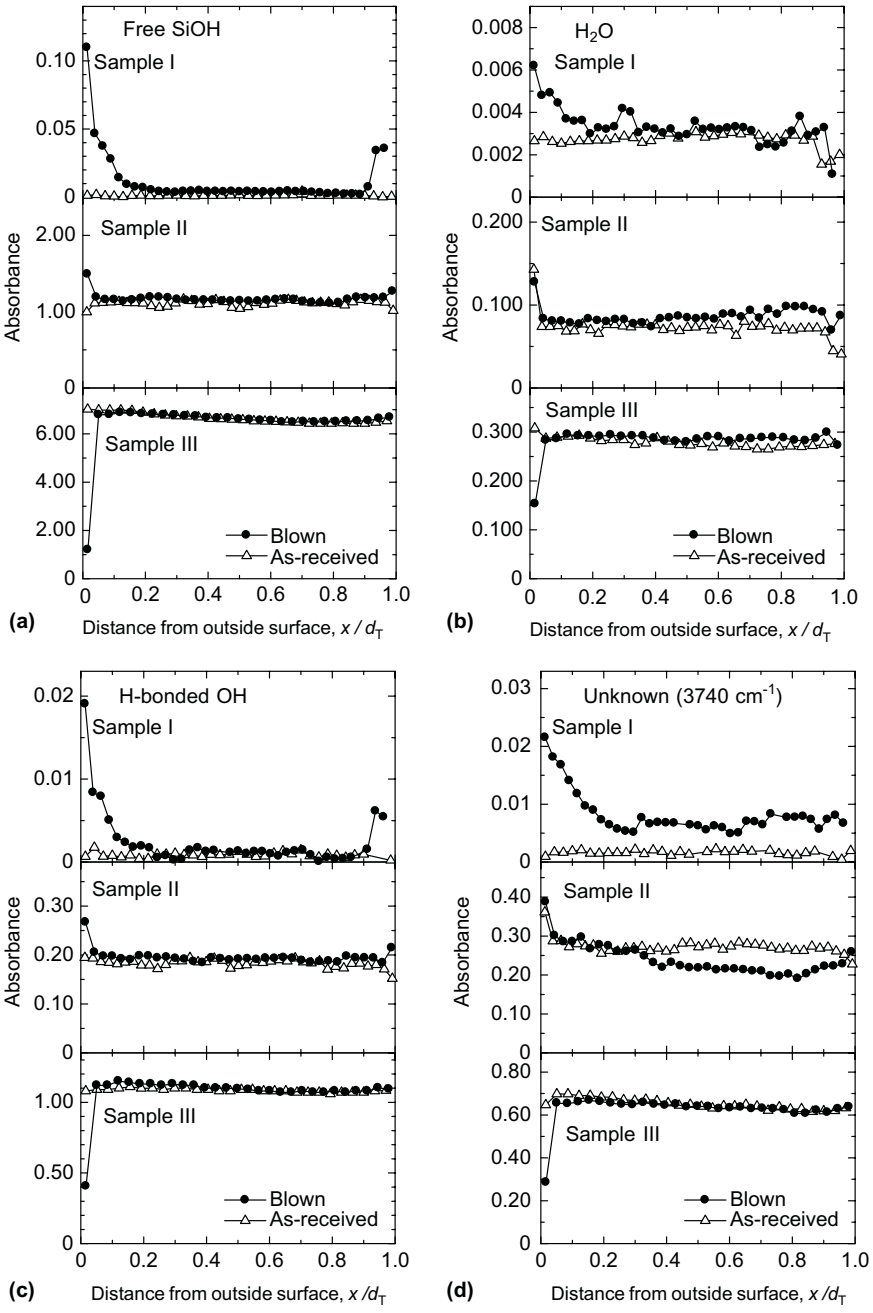

Fig. 5. Distributions of decomposed OH components: (a) 3661 cm^{-1} band due to free OH, (b) 3426 cm^{-1} band due to H_2O, (c) 3551 cm^{-1} band due to H-bonded OH, (d) 3740 cm^{-1} band due to an unknown component.

slightly decreased with increasing proximity to the ISS, both before and after blowing. The ratio of the peak intensity of H_2O to that of the free SiOH components in Sample II is 0.07–0.1 before blowing. Although the character of the distribution of the H_2O/free SiOH intensity ratio of the blown tubes is similar to that of the as-received tube, slight differences are observed. The ratio in the blown tubes at the OS and in the bulk are not significantly different, but the ratio at the OS in the as-received tube is approximately two times greater than that in the bulk. Moreover, the ratio in the blown tube increases slightly with increasing x in the bulk region.

In Sample III, the amount of H_2O is approximately constant, and almost no change was observed upon blowing except near the OS. Near the OS, the ratio increased above that in the bulk, indicating that the decrement of the free SiOH is greater than that of H_2O. Upon blowing, the OH content decreased markedly within 50 μm ($x/d_T \approx 0.02$) of the OSS. The ratio of the intensity of H_2O to that of the free SiOH components is 0.05 both before and after blowing.

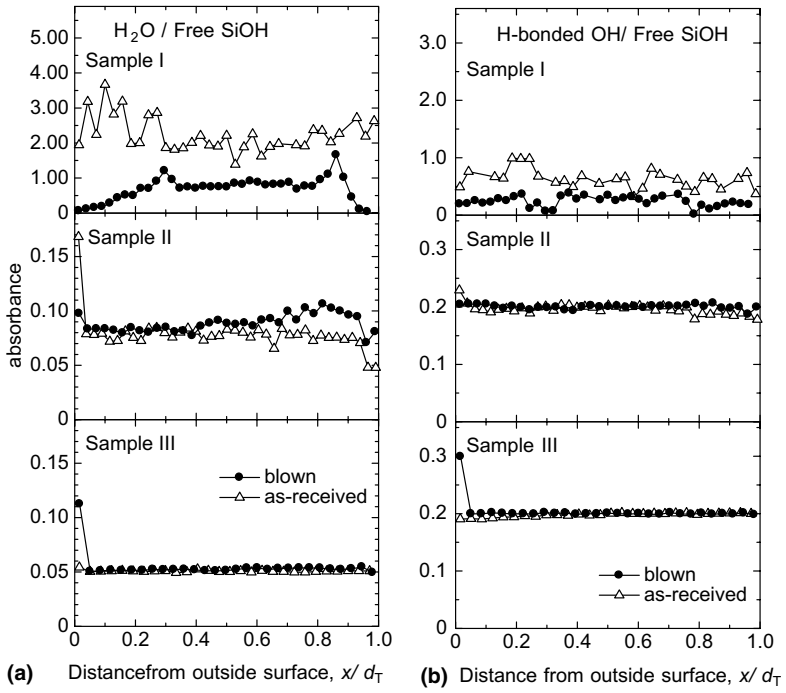

Fig. 6. Distribution of the peak intensities of the (a) H_2O band at 3426 cm^{-1} and (b) the hydrogen-bonded band at 3551 cm^{-1} relative to that of the free Si–OH band at 3661 cm^{-1}.

Fig. 5(c) shows the distribution of the intensity of the 3551 cm^{-1} band due to the hydrogen-bonded OH. Although the intensities of the H-bonded components are weaker than those of free OH, they are distributed almost proportionally to those of free SiOH. The ratios of the intensity of H-bonded SiOH to that of the free SiOH components are 0.2 in Samples II and III before and after blowing, except at the OSS in the blown samples (Fig. 6(b)).

We assumed an absorption component at 3740 cm^{-1}, as shown in Fig. 5(d), whose origin is unknown. This component was required in order to reproduce the shoulder at 3740 cm^{-1} in Fig. 4. The intensity increased gradually with increasing proximity to the OSS in Sample I.

3.2. Change of fictive temperature distribution

Agarwal et al. found that the fictive temperature T_F of v-SiO_2 can be determined on the basis of the peak position of IR absorption at ≈2260 cm^{-1} [12], irrespective of the type of v-SiO_2, from the following relation:

$$T_F = \frac{43\,809.21\ \mathrm{K\,cm^{-1}}}{n - 2228.64\ \mathrm{cm^{-1}}}. \quad (1)$$

Since the fictive temperature is sensitive to the peak position, the peak position was determined by the peak position of a second-order curve that have been fitted within 40 cm^{-1} around the peak in order to reduce the error of the determination of the peak wavenumber.

The distributions of fictive temperature before and after blowing are shown in Fig. 7. The fictive temperature of the as-received Sample I is a constant value at ≈1420 K, except near the OSS. The fictive temperature increases by almost 200 K upon blowing, and reaches a maximum at $x \approx 1000\,\mu m$ ($x/d_T \approx 0.27$). The fictive temperatures of Samples II and III are almost constant throughout the cross-section and no changes are ob-

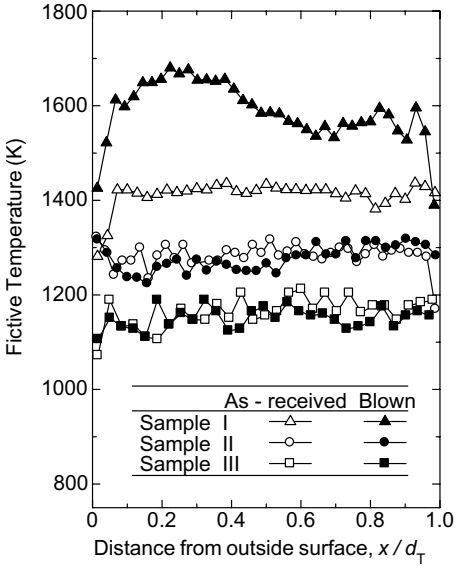

Fig. 7. Distributions of the fictive temperature before and after blowing.

served upon blowing. The only exception is seen in the as-received Sample II at the ISS, at which the value of the fictive temperature is found to be lower than that in the bulk.

4. Discussion

4.1. Distribution of OH content

Upon blowing, the amount of free SiOH, hydrogen-bonded OH, and H_2O in Samples I and II increased within approximately 500 μm ($x/d_T \approx 0.14$) of the OS. These hydroxyl structures are considered to be introduced from the H_2O vapor in the hydrogen–oxygen flame. Near the OSS in Sample III, on the other hand, the number of hydroxyl structures decreased markedly. These findings suggest that the creation of the hydroxyl group occurs when there is an equilibrium between the introduction of hydroxyl from the H_2O vapor and the diffusion of hydroxyls from the material.

The H_2O molecules are considered to diffuse into the glass network. Some H_2O molecules can diffuse directly by conserving their molecular structure, but most molecules must diffuse by reaction with the SiO_2 glass network in the following manner:

$$\equiv Si{-}O{-}Si\equiv + H_2O \rightleftharpoons \equiv Si{-}OH + HO{-}Si\equiv \quad (2)$$

The equilibrium value of the OH content is considered to depend on the vapor pressure in the flame and the temperature. The equilibrium value of the OH content in the blowing process is considered to be between those of Samples II and III because the sign of the changes of the OH content near the surface upon blowing are opposite.

Near the ISS, the amount of free SiOH and hydrogen-bonded OH increased slightly in Samples I and II. Since these surfaces were not fused by a burner, some form of water must diffuse into the inner part during blowing. Two possibilities for the origin of this water can be considered: one is the H_2O molecules adsorbed on the IS, and another is H_2O vapor in the nitrogen gas flowed into the tube.

The flame in the blowing also contains hydrogen molecules. Therefore it might react with the glass network to form hydrides in addition to the hydroxyl as expressed by

$$\equiv Si{-}O{-}Si\equiv + H_2O \rightleftharpoons \equiv Si{-}OH + H{-}Si\equiv \quad (3)$$

If the SiH structures introduced by the process expressed in Eq. (3), a peak at $\approx 2250\,cm^{-1}$ must be induced [13]. One might suspect that this peak interferes the determination of the fictive temperature because this peak exists near the peak at $\approx 2260\,cm^{-1}$ using the determination of the fictive temperature. The molar extinction coefficient of this band is reported to be $351\,mol^{-1}\,cm^{-1}$ [13]. The peak intensities of this band are $\approx 0.2\,cm^{-1}$ throughout the cross-section in all samples before and after blowing. The hydride concentration of a sample similar to Sample I is reported to be $\approx 2\times 10^{18}\,cm^{-3}$, based on the intensity of a Raman band at $2270\,cm^{-1}$ [14]. The estimated value of the $2250\,cm^{-1}$ band intensity in that sample is $0.7\times 10^{-3}\,cm^{-3}$, which is two orders smaller than that of the $2260\,cm^{-1}$ band. Upon blowing, the increment of the SiH is at most the increment of SiOH structure if all SiH structure is introduced by the process expressed in Eq. (3). The increment of SiOH in Sample I is $3\times 10^{19}\,cm^{-3}$ (400 ppm), which causes the absorption intensity of $0.01\,cm^{-1}$ at $2250\,cm^{-1}$. Even in this case, this intensity is approximately 20 times less than that of the $2260\,cm^{-1}$ band. The amount of the SiH introduced by the blowing, however, must be much less than that of SiOH, and the intensity of the SiH component should be negligible compared to that of the $2260\,cm^{-1}$ band. Since the intensity of the $2270\,cm^{-1}$ Raman band of SiH in the present sample is difficult to determine due to its very weak intensity, we did not measure the SiH concentration.

Fig. 5 indicates that the intensities of the free SiOH, H_2O and hydrogen-bonded OH peaks of the blown Samples II and III at the OS are almost of the same magnitude. This finding suggests that the reactions between the gases in the flame and the Si–O–Si bonds are in equilibrium at the OS. Although the fractions of the increment of the hydroxyl components in Sample I near the OS are greater than those of the increment in the other samples, the absolute values of the hydroxyls in Sample I near the OSS are still less than those of the other samples. The value of the OH content at the outermost part of Sample III is 2.5 times greater than that in Sample I, even though we assumed an equilibrium in OH content. However, the outermost measurement point is about ≈50 μm from the OS. Therefore, the true value of the OH concentration of the samples at the OS must be nearer value than these measurement values. These values cannot be the same because the system had not reached equilibrium; at the equilibrium, the OH content throughout the cross-section must be constant. Since Sample I has almost no OH, a high strain and therefore stress might be induced by the introduction of hydroxyl groups through fusing. The stress is considered to promote the increment of the OH content in Sample I. In Sample III, on the other hand, higher value of OH reduces the increment of the stress in the inner parts, and the region where the OH changed might be narrower.

The ratios of the intensity of hydrogen-bonded SiOH to that of free SiOH components, ≈0.2, are almost the same in Samples II and III. This finding indicates that some amount of SiOH must be hydrogen bonded to oxygen atoms in a ≡Si—O—Si≡ structure [11], and that

free SiOH and hydrogen-bonded OH must be in equilibrium. The only exception is near the OS in Sample III, where the ratio of the intensity of the hydrogen-bonded SiOH to that of the free SiOH components was larger than that in the bulk, as seen in Fig. 6(b). The increment of this ratio at the OSS in Sample III is due to the decrement of the amount of free SiOH near the surface; the amount of hydrogen-bonded SiOH was not changed as much as that of free SiOH. This finding suggests that upon blowing, the hydrogen-bonded SiOH is rendered more stable than free Si–OH in Sample III. The ratio of the amount of the hydrogen-bonded SiOH to that of the free SiOH in Sample I is larger and has much more error than the ratios in the other samples. This is simply because the amount of free SiOH in Sample I is far less than that in the other samples.

4.2. Fictive temperature distribution

The difference in fictive temperature among Samples I, II, and III may be due to the difference in the relaxation time of the silica glass structure, which strongly depends on the OH content. For example, the structural relaxation time evident from Raman bands at 495 (D_1) and 606 cm^{-1} (D_2) of v-SiO_2, which contains 1000 ppm of OH, is three orders greater than that in OH-free v-SiO_2 [15].

The fictive temperature of the as-received Sample I was 1420 K, which is near the strain temperature of ≈1420 K [2]. The fictive temperature of Sample I decreased steeply with increasing proximity to the OS in both the as-received and blown tubes. This is because the structure at the surface in Sample I could relax more rapidly than that in the bulk [16]; therefore, the structure near the surface could relax to a lower fictive temperature during the tube drawing and glass blowing processes. In the glass blowing process, the introduction of the OH structure promotes the relaxation of the structure [16]. The fictive temperature of Sample I is an increasing function of x in the region x = 0–900 μm ($x/d_T \approx 0-0.26$), and reaches a maximum at ≈1000 ($x/d_T \approx 0.28$) μm from the OSS. Furthermore, the fictive temperature decreases gradually with increasing the proximity the ISS, and it becomes a constant value at $x \approx$ 2200 ($x/d_T \approx 0.6$) μm. This distribution of the fictive temperature reflects the distribution of the temperature during blowing with the hydrogen–oxygen flame.

Samples II and III have shorter relaxation times than Sample I, because their OH contents are higher than that in Sample I. Therefore, the structure of Samples II and III can be relaxed to lower fictive temperatures during cooling in both the tube drawing and blowing processes. The difference in fictive temperature between the surface and bulk within Samples II and III is small, because their relaxation times are relatively short compared to their cooling rates. In particular, the relaxation time of Sample III is the shortest among the samples. Thus, the fictive temperature of Sample III becomes approximately constant throughout its cross-section.

5. Summary and conclusion

Structural changes upon blowing with a hydrogen–oxygen flame in the cross-sections of three types of silica glass tubes were studied by means of microscopic spectroscopy. These samples, referred to as Samples I, II and III, contain <1, 200, and 1200 ppm of OH, respectively.

The OH contents of Samples I and II increased within 1000 μm of the surface upon blowing, but decreased steeply at the OS in Sample III. The peak decomposition of the IR absorption demonstrates that most of the OH is in the form of free SiOH. At the OS, the amount of free SiOH changed markedly in every sample. The amounts of hydrogen-bonded OH and H_2O decreased in Sample III at the OS, but they remained almost constant in Samples I and II. At the ISS of Sample I, the intensities of the peaks of these components were too small to demonstrate any change upon blowing. At the IS, the amount of H_2O in Sample II increased, but in Sample III it did not.

The fictive temperature of the as-received Sample I was 1420 K, which is near the strain temperature of ≈1420 K. The fictive temperature of Sample I increased upon blowing and took a maximum at $x \approx 1000$ μm from the OS. The fictive temperatures of blown Samples II and III remained almost the same as those in the as-received samples, except near the OSS in Sample II.

Upon blowing, the fictive temperature in the cross-section of the tube did not change in the OH-containing tube. The OH content near the surface increased in the samples with no OH and with 200 ppm OH, while in the sample with 1300 ppm, the OH content decreased. These results suggest the possibility of obtaining a stable sample by blowing, i.e., because the fictive temperature and OH content remain constant, using a silica glass tube containing an appropriate amount of OH. The optimal OH content is considered to be between 200 and 1300 ppm.

References

[1] R. Brückner, J. Non-Cryst. Solids 5 (1970) 123.
[2] H. Kawazoe, K. Awazu, Y. Ohki, N. Kuzuu, S. Todoroki, A. Hayashi, H. Fukuda (Eds.), Hishoushitsu Shirika Zairyou Ouyou Handobukku (Handbook for Application of Amorphous Silica), Realize, Tokyo, 1999.
[3] D.L. Griscom, J. Ceram. Soc. Jpn. 99 (1991) 923.
[4] L. Skuja, J. Non-Cryst. Solids 239 (1970) 123.
[5] N. Kuzuu, Y. Kokubo, I. Serizawa, L.-H. Zeng, K. Fujii, M. Yamaguchi, K. Saito, A.J. Ikushima, J. Non-Cryst. 333 (2004) 115.

[6] N. Kuzuu, Reza Kenkyu (Rev. Laser Eng.) 23 (1995) 396 (in Japanese).
[7] N. Kamisugi, N. Kuzuu, Y. Ihara, T. Nishimura, Jpn. J. Phys. 36 (1997) 6785.
[8] N. Kuzuu, J.W. Foley, N. Kamisugi, J. Ceram. Soc. Jpn. 106 (1998) 525.
[9] T. Nishimura, I. Serizawa, N. Kuzuu, J. Ceram. Soc. Jpn. 108 (2000) 1034.
[10] G. Hetherington, K.H. Jack, Phys. Chem. Glass 3 (1962) 129.
[11] A. Agarwal, M. Tomozawa, J. Non-Cryst. Solids 220 (1997) 178.
[12] A. Agarwal, K.M. Davis, M. Tomozawa, J. Non-Cryst. Solids 191 (1995) 185.
[13] J.E. Shelby, J. Appl. Phys. 50 (1979) 3702.
[14] N. Kuzuu, H. Horikoshi, T. Nishimura,, Y. Kukubo, J. Appl. Phys. 93 (2003) 9062.
[15] F.L. Galeener, J. Non-Cryst. Solids 71 (1985) 373.
[16] M. Tomozawa, Y.-L. Peng, A. Agarwal, Jpn. J. Appl. Phys. Suppl. 37 (1) (1998) 1.